EVALUATION OF QRS-COMPLEX DETECTION ON REAL-TIME ECG DATA USING A MICROCONTROLLER

ĐÁNH GIÁ KHẢ NĂNG PHÁT HIỆN PHỨC BỘ QRS TRÊN DỮ LIỆU ECG ĐO THỜI GIAN THỰC BẰNG VI ĐIỀU KHIỂN

Tran Thanh Luan[1,2], Tran Vy Khang[3], Nguyen Quy Hung[3], Nguyen Tien Thanh[3], Nguyen Chi Ngon[3], Nguyen Van Khanh[3]*

[1]PhD student in Control and Automation engineering, College of Engineering, Can Tho University, Vietnam
[2]Vinh Long University of Technology Education, Vietnam
[3]College of Engineering, Can Tho University, Vietnam

*Corresponding author: vankhanh@ctu.edu.vn

(Received: June 07, 2025; Revised: July 21, 2025; Accepted: September 08, 2025)

DOI: 10.31130/ud-jst.2025.23(9A).305

Abstract - Nowadays, electrocardiogram (ECG) signals play an important role in the diagnosis of cardiovascular diseases. Detecting the QRS complex in ECG is essential, because it best represents the pathological condition of the heart. This study evaluates the ability to detect QRS on real-time ECG data using a microcontroller (MCU). An 8-channel ECG signal acquisition system was built based on the ADS1292 chip and ESP32 MCU. ECG data were collected from volunteers and tested with three QRS detection algorithms: Pan-Tompkins, Hilbert Transform and Englese & Zeelenberg applied on the second channel. The corresponding accuracy results reached 100%, 99.46% and 99.63%, with processing times of 117 µs, 116 µs and 222 µs, respectively. This study demonstrates the effectiveness of the direct ECG collection and analysis system on MCU, and creates a platform for the development of mobile cardiovascular diagnostic devices, helping with early detection and improving the quality of public health care.

Key words - ECG; QRS; Pan-Tompkins; Hilbert Transform; Englese & Zeelenberg

Tóm tắt - Ngày nay, tín hiệu điện tâm đồ (ECG) giữ vai trò quan trọng trong chẩn đoán các bệnh tim mạch. Việc phát hiện phức bộ QRS trong ECG là rất cần thiết, vì nó biểu hiện rõ nhất tình trạng bệnh lý của tim. Nghiên cứu này đánh giá khả năng phát hiện QRS trên dữ liệu ECG đo thời gian thực bằng vi điều khiển (VĐK). Một hệ thống thu thập tín hiệu ECG 8 kênh được xây dựng dựa trên chip ADS1292 và VĐK ESP32. Dữ liệu ECG được thu từ các tình nguyện viên và thử nghiệm bằng ba thuật toán phát hiện QRS là Pan-Tompkins, Hilbert Transform và Englese & Zeelenberg áp dụng trên kênh thứ 2. Kết quả độ chính xác tương ứng đạt 100%, 99,46% và 99,63%, với thời gian xử lý lần lượt là 117 µs, 116 µs và 222 µs. Nghiên cứu này chứng minh hiệu quả của hệ thống thu thập và phân tích ECG trực tiếp trên VĐK, đồng thời tạo nền tảng phát triển các thiết bị chẩn đoán tim mạch di động, giúp phát hiện sớm và nâng cao chất lượng chăm sóc sức khỏe cộng đồng.

Từ khóa - ECG; QRS; Pan-Tompkins; Hilbert Transform; Englese & Zeelenberg

1. Introduction

Electrocardiogram (ECG) is a commonly and effectively used diagnostic tool in the field of cardiology [1]. Within the ECG signal, the QRS complex plays a particularly important role, as it clearly reflects the contractile activity of the heart, thereby enabling the detection of abnormalities [2]. Therefore, accurate detection and localization of the QRS complex is a critical step in ECG signal analysis [3]. Parameters related to the QRS complex, such as amplitude, duration, width, and waveform, are utilized to assess cardiovascular status, determine heart rate, and diagnose cardiac diseases [4], [5].

Numerous studies have proposed improvements and new methods for automatic QRS detection. These studies mainly focus on two objectives: enhancing the accuracy of detection algorithms and reducing latency to enable real-time applications. Entisar et al. [6] employed the AD8232 sensor and ESP8266 Node to collect data, which was then transferred to a computer for processing and analysis using MATLAB R2021B software combined with the Pan-Tompkins (PT) algorithm to detect the QRS complex. Imtiaz et al. [7] proposed a solution using PT++, which can distinguish between R peaks and noise, thereby improving ECG signal classification and identification. This method reduced false positives by 2.8% and false negatives by 1.8%, while also decreasing processing time by 33%. In addition to PT, many other studies have utilized time-frequency transformations and signal filtering techniques for QRS detection. The Hilbert Transform (HT) has also been applied to effectively detect QRS complexes and locate R peaks without the need for fixed amplitude thresholds [8]. Wavelet-based methods are widely used, allowing for noise filtering and extraction of QRS features across different frequency bands [8], [9]. Rakshit et al. [8] used wavelets to eliminate noise and combined HT to identify R peaks, achieving an accuracy of approximately 99.83%. This study employed the MIT-BIH dataset, which is a publicly available dataset collected and processed under ideal conditions. This poses limitations for practical deployment when signals are collected directly in various noisy environments. Lourenço's study [10] combined the offline Englese & Zeelenberg (E-Z) method with Christov's online adaptive threshold and tested it on fingertip ECG signals. When evaluated using data from the commercial bioPLUX device, the algorithm achieved an average valid percentage of 94.5%. However, this

algorithm was limited to fingertip ECG signals and has not yet been applied to standard ECG measurements.

Currently, embedded systems are increasingly advancing, and microcontrollers (MCUs) play a crucial role in applying research on classification and QRS detection on ECG [11], [12] due to advantages such as compactness, portability, and the ability to directly acquire signals, thereby minimizing latency. However, implementation on MCUs presents challenges due to limited resources and memory, affecting the application of complex algorithms. Recent studies have demonstrated the feasibility of deploying QRS detection algorithms on MCUs, such as the work by Kouekeu et al. [11], who developed algorithms for the ESP32 and Arduino Nano MCUs. They achieved F1-scores of 99.75% on the MIT-BIH Arrhythmia dataset and 97.39% on the MIT-BIH Noise Stress Test, with processing times of 3.38 µs per sample on ESP32 and 383 µs on Arduino Nano. Sinha's study [12] proposed an algorithm implemented on the STM32F4VE MCU for QRS detection, achieving a detection performance of approximately 99.7%. These studies were mainly tested on publicly available databases, with limited surveys conducted on real-world signals.

In general, AI-based solutions, although highly accurate, are complex and pose many challenges. In contrast, traditional algorithms such as PT, HT, and E-Z are simple in structure, operate stably, offer high accuracy, fast processing, and are suitable for direct deployment on MCUs. These algorithms only employ basic operations, ensuring real-time ECG signal processing performance directly on MCUs. The results of implementing and evaluating these algorithms will serve as a foundation for integrating machine learning in future cardiovascular disease diagnosis. Therefore, the objective of this study is to develop a compact embedded system using the ESP32 MCU to directly acquire and process multi-channel real-time ECG data. QRS detection algorithms such as PT, HT, and E-Z will be implemented, evaluated, and compared on ECG signals collected from a group of volunteers. The most effective algorithm will be identified, providing a basis for developing mobile devices capable of early detection and diagnosis of cardiovascular abnormalities in practical settings.

2. Research methods

This study is an experimental investigation aimed at evaluating the effectiveness of QRS complex detection in real-time ECG signals using an embedded system based on the ESP32 MCU. The acquired ECG data are stored directly onto a microSD card, followed by preprocessing for noise filtering. Subsequently, the signals are analyzed using the PT, HT, and E-Z algorithms to identify QRS complexes and R peaks. The performance of these algorithms is assessed based on accuracy (ACC), sensitivity (Se), positive predictive value (+P), and detection error rate (DER). The collected data are processed using descriptive statistical methods, calculating mean and standard deviation values with Minitab software - a powerful tool for statistical analysis, data processing, and detailed scientific visualization - thereby identifying the most suitable algorithm for practical applications.

2.1. Data acquisition circuit and QRS detection algorithm testing

ECG signals are collected using the ADS1298ECG-FE signal processing circuit in combination with standard electrodes attached to the subject. This integrated circuit can directly measure 8 channels of ECG from electrodes, including Lead I, Lead II (LII), V1, V2, V3, V4, V5, and V6. In this study, only LII is utilized. The sampling rate is 500 Hz. Data are sequentially filtered using high-pass (HPF) and low-pass (LPF) filters to eliminate noise induced by power lines, body movement, muscle tension, and other high-frequency interferences. After filtering, algorithms are applied to detect QRS complexes. The results from these algorithms are stored for evaluation and comparison.

The block diagram is presented in Figure 1. In this diagram, the signal acquisition block consists of ECG signal cables with 10 leads, connecting 6 chest electrodes and 4 limb electrodes. The signals are processed by the ADS1298ECGFE Rev C module, a 24-bit ADC converter with an integrated programmable-gain amplifier (PGA). The control block utilizes the ESP32 MCU with a dual-core CPU. The data storage block employs a high-capacity SD card connected to the ESP32 via SPI interface. The display block uses a 3.2-inch ILI9341 TFT LCD to display real-time ECG signals, facilitating monitoring during experiments. The power block uses a Li-ion battery combined with a voltage regulation circuit to provide stable power for the entire system.

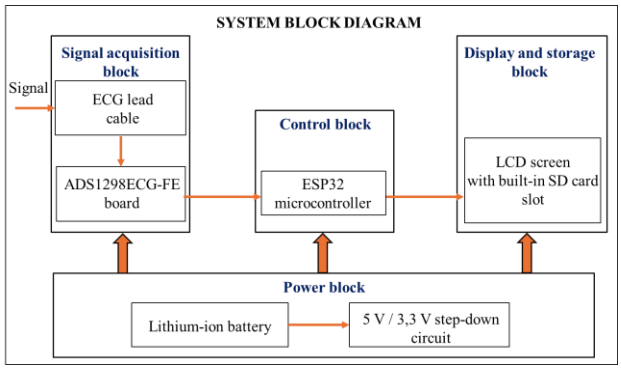

Figure 1. *System block diagram*

2.2. Signal filtering

As described, noise during measurement is filtered using both LPF and HPF. The LPF has a cutoff frequency of 40 Hz to remove high-frequency and power line noise, while the HPF is designed with a cutoff frequency of 0.5 Hz to eliminate ultra-low frequencies caused by poor electrode-to-skin contact and movement or muscle tension. Both filters are applied in real time to ECG data from the electrodes. To increase the slope of the response and balance computation time, the LPF utilizes a fourth-order transfer function, and the HPF uses a second-order transfer function. These filters are mathematically represented in equations (1) and (2):

$$y[n] = \sum_{k=0}^{2} b_k x[n-k] - \sum_{k=1}^{2} a_k y[n-k] \quad (1)$$

$$y[n] = \sum_{k=0}^{4} b_k x[n-k] - \sum_{k=1}^{4} a_k y[n-k] \quad (2)$$

where, a_k and b_k are coefficient vectors designed with the following values:

- HPF

a_k = [*-1.991114378 0.991153657*]

and b_k = [*0.99567033 -1.991134067 0.99567033*]

- LPF

a_k = [*-2.717593123 2.911990841 -1.431263441 0.270105198*]

and b_k = [*0.002077467 -0.0083098 0.012464803 0.008309868 0.008309868*]

Figure 2 illustrates the amplitude and phase responses of the designed HPF and LPF filters.

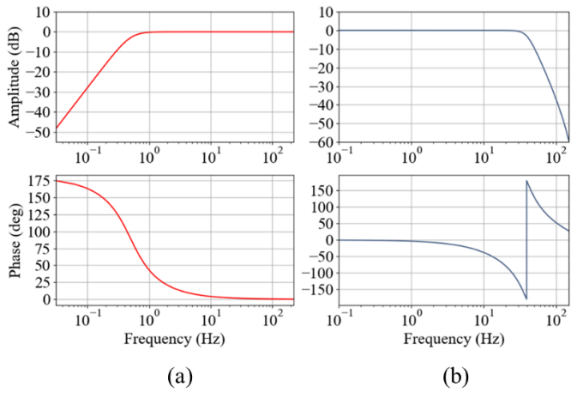

Figure 2. *Amplitude and phase responses of: (a) HPF and (b) LPF*

The responses show that the signal amplitude is reduced by 20 dB at the designed cutoff frequency. The LPF exhibits a steep amplitude response, effectively eliminating noise above 40 Hz while preserving ECG characteristics.

2.3. QRS complex detection algorithms

Figure 3 depicts the signal processing steps performed on the ESP32 MCU.

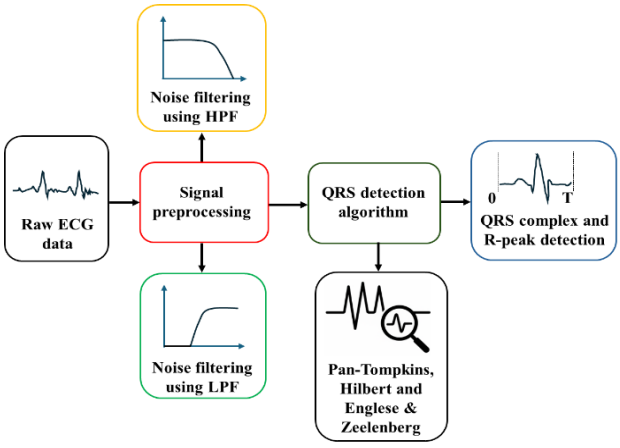

Figure 3. *ECG signal processing procedure on ESP32*

In this study, three algorithms - PT, HT, and E-Z - are implemented to detect QRS complexes in real time using the LII ECG data stream acquired from the sensor. As previously mentioned, only LII is used for QRS detection algorithm evaluation. The ECG data stream is first denoised using HPF and LPF filters before entering the QRS detection block via the three aforementioned algorithms. The output of the QRS detection block is the R peak location and an ECG cycle ready for further analysis or recognition applications. The mathematical details of the three QRS detection algorithms used are as follows:

2.3.1. Pan-Tompkins algorithm

The PT algorithm [13], developed in 1985 by John Pan and Willis J. Tompkins, is carried out in three main steps. First, the filtered signal is differentiated to highlight abrupt changes [13], [14]. Differentiation emphasizes the signal slope, especially at R peaks, while reducing the influence of P and T waves. Differentiation is performed according to equation (3):

$$d(nT)=\frac{-x(nT-2T)-2x(nT-T)+2x(nT+T)+x(nT+2T)}{8T} \quad (3)$$

where x is the filtered ECG signal at time nT and T is the sampling period.

The differentiated signal is squared to amplify the QRS complex [13], as shown in equation (4):

$$s(nT)=\left[d(nT)\right]^2 \quad (4)$$

Subsequently, the signal is passed through a moving average filter to smooth the squared signal [14], as in equation (5). This filter reduces random noise and enhances signal stability, facilitating easier R peak detection.

$$M(nT)=\frac{1}{N}\sum_{k=0}^{N-1}s(nT-kT) \quad (5)$$

where N is the number of samples in a sliding window ($N = 15$) and k is the sample index.

Finally, $M(nT)$ is subjected to an adaptive threshold based on the processed signal to identify R peaks. This threshold enables accurate QRS complex detection in the signal.

2.3.2. Hilbert transform-based algorithm

The HT algorithm is also used to detect and identify key features of the QRS complex [15]. This technique generates a complex signal from the original, enabling precise determination of instantaneous phase and amplitude. According to [16], the HT is mathematically represented as equation (6):

$$\hat{x}(t)=H\left[x(t)\right]=\frac{1}{\pi}\int_{-\infty}^{\infty}x(\tau)\frac{1}{t-\tau}d\tau \quad (6)$$

where $x(t)$ is the signal to be transformed - in this study, the real-time ECG signal sampled from electrodes. To implement equation (6) for real-time signal segmentation at the input $x(t)$, convolution with $(\pi t)^{-1}$ yields equation (7):

$$\hat{x}(t)=\frac{1}{\pi t}x(t) \quad (7)$$

Applying the forward FFT to both sides gives equation (8):

$$F\left\{\hat{x}(t)\right\}=\frac{1}{\pi}F\left\{\frac{1}{t}\right\}F\left\{x(t)\right\} \quad (8)$$

With $F\left\{\frac{1}{t}\right\}=\int_{-\infty}^{\infty}\frac{1}{x}e^{-i2\pi fxdx}=-j\pi(\operatorname{sgn} f)$, substituting into (8) yields equation (9):

$$F\left\{\hat{x}(t)\right\}=-j(\operatorname{sgn} f)F\left\{x(t)\right\} \quad (9)$$

Or: $$F\{\hat{x}(t)\} = -j(\operatorname{sgn} f)\sum_{n=0}^{N-1} x(t)e^{\frac{-j2\pi n}{N}} \quad (10)$$

For discrete signals in the frequency domain at each angular frequency $\omega_k = 2\pi k/N$, calculations for $-j\pi(\operatorname{sgn} f)$ are performed according to equation (11) [14].

$$-j(\operatorname{sgn} f) = \begin{cases} -j & \text{when } \omega_k > 0 \\ 0 & \text{when } \omega_k = 0 \\ j & \text{when } \omega_k < 0 \end{cases} \quad (11)$$

After classifying angular frequencies ω_k, the inverse Fourier transform (IDFT) is applied to return the frequency-domain discrete signal to the time domain. The IDFT employs functions proposed by [17] and is implemented according to equation (12):

$$\hat{x}(nT) = F^{-1}(X) = \frac{1}{N}\sum_{n=0}^{N-1} X(F)e^{\frac{j2\pi n}{N}} \quad (12)$$

Both $x(nT)$ and $x\text{-}hat(nT)$ are used to determine the signal envelope according to equation (13):

$$Envelope = \sqrt{x(t)^2 + \hat{x}(t)^2} \quad (13)$$

The envelope is a curve representing the amplitude variation of the ECG signal over time, highlighting key features of the ECG signal [14], [15]. It is then used to locate the R peak based on a dynamic threshold as previously described.

2.3.3. Engelse & Zeelenberg algorithm

In addition to the above algorithms, E-Z is also a proposed method for QRS complex detection, designed for efficient operation on ECG signals [10]. This method employs filtering and signal analysis steps to emphasize QRS complex features, ensuring accurate detection even in noisy signals. First, the filtered ECG signal undergoes discrete differentiation $y_1[nT]$ as in equation (14):

$$y_1[n] = x[n] - x[n-4] \quad (14)$$

Next, $y_1[n]$ is smoothed by LPF according to equation (15):

$$y_2[n] = \sum_{i=0}^{4} c_i y_1[n-i] \quad (15)$$

Here, $c_i = [1\ 4\ 6\ 4\ 1]$ highlights peak waves in the differentiated signal, facilitating more precise R peak detection.

2.3.4. Dynamic threshold detection algorithm

After applying one of the above algorithms, the ECG signal is used to detect QRS complexes by locating the R peak. In this study, the R peak is detected using an adaptive threshold determined by the algorithm proposed by Utomo, 2017 [18]. A sliding window containing 100 data samples shifts one sample to the right each time. With each shift, the maximum value in the window (Peak) is identified to update the threshold according to equation (16):

$$Threshold = \alpha\gamma Peak - (1-\alpha)Threshold \quad (16)$$

where, α is the threshold smoothing coefficient, ranging from 0 to 1, providing flexibility in threshold updates, and γ is the scaling constant, adjusting the threshold sensitivity to the maximum value in the sliding window.

Applying the threshold to the output signals of the PT, HT, and E-Z algorithms optimizes QRS detection, enabling effective and accurate R peak identification. By adjusting the threshold to suit each signal and specific situation, QRS detection capability is significantly improved. Within an ECG cycle, only one data point $x[n]$ is considered the R peak of the complex if the values on both sides of $x[n]$ are smaller than itself and all are greater than the threshold as represented in equation (17).

$$x[n] > x[n-1], x[n] > x[n+1], x[n] > Threshold \quad (17)$$

2.4. Experimental setup for algorithm evaluation

The experiment was conducted at the PLC and Industrial IoT Engineering Laboratory, Can Tho University. Its purpose was to implement and evaluate the QRS complex detection capability of the algorithms combined with dynamic thresholding. The experiment was designed as a trial study, with the main objective of assessing the QRS detection capability of the PT, HT, and E-Z algorithms on the MCU. Therefore, the experiment involved a group of 10 student volunteers from Can Tho University. The volunteers were male, aged 21–22, in good health to ensure physiological consistency and facilitate repeated measurements, meeting the minimum requirements for experimental studies evaluating device and signal processing algorithm performance. The experimental setup is illustrated in Figure 4. Volunteers lay on a table and were connected to two groups of electrodes: chest electrodes (1) attached at points V1–V6 and limb electrodes (2) clamped to both arms and legs. The ECG signal cables (3) connected the electrodes to the real-time ECG signal acquisition and processing device (4). During algorithm execution, volunteers were asked to remain still to avoid motion artifacts. The table position was arranged to minimize power line interference. Each volunteer was measured four times, with one volunteer measured five times as backup in case of data errors; each measurement lasted 30 seconds, resulting in a total of over 1400 heart cycles, meeting the ANSI/AAMI EC57 standard recommendation (≥ 1,000 beats) for estimating Se and +P with an error margin of ±1%–1.5% at a 95% confidence level [19]. Data collected from 8 ECG channels were stored on a microSD card for evaluation.

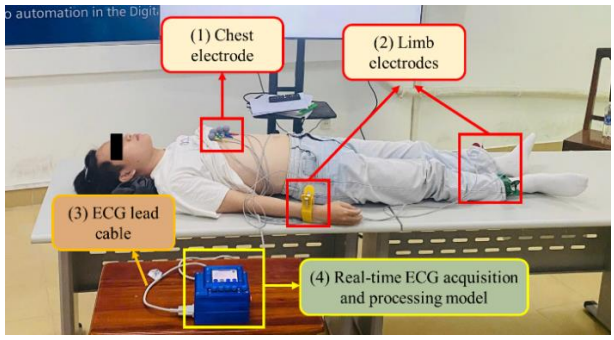

Figure 4. *Experimental Setup and Data Acquisition*

2.5. Evaluation criteria

The PT, HT, and E-Z algorithms were applied to the same dataset of collected ECG signals, and results were

compared based on accuracy (ACC), sensitivity (Se), positive predictive value (+P), and detection error rate (DER). These metrics are defined by equations (18), (19), (20), and (21):

$$\mathrm{Se} = \left(\frac{TP}{TP+FN}\right)\times 100\% \quad (18)$$

$$+P = \left(\frac{TP}{TP+FP}\right)\times 100\% \quad (19)$$

$$DER = \left(\frac{FP+FN}{TotalBeats}\right)\times 100\% \quad (20)$$

$$Acc = 100\% - DER \quad (21)$$

where, *TP* is the number of ECG cycles with correctly detected R peaks located within the Q to S interval. *FP* is the number of cycles with incorrectly detected R peaks outside the QRS region. *FN* is the number of missed R peaks between QRS cycles, and *TotalBeats* is the total number of QRS cycles present in the collected ECG segment.

3. Results and discussion

After conducting the experiments, a total of 41 segments of LII and other channel data were stored. These datasets were manually reviewed to assess the integrity of the QRS complexes by the research team, following recommended standards for QRS complex identification. The results were cross-checked to detect and resolve any inconsistencies. Although there was no direct involvement from cardiology specialists, the research team referenced standard documents and guidelines for ECG wave identification to ensure objectivity and the highest reliability for the reference dataset used to evaluate algorithm performance. In total, 1,470 complete QRS complexes on LII were used for real-time testing with the selected algorithms.

Raw LII ECG signals were collected and processed using HPF and LPF filters, as shown in Figure 5.

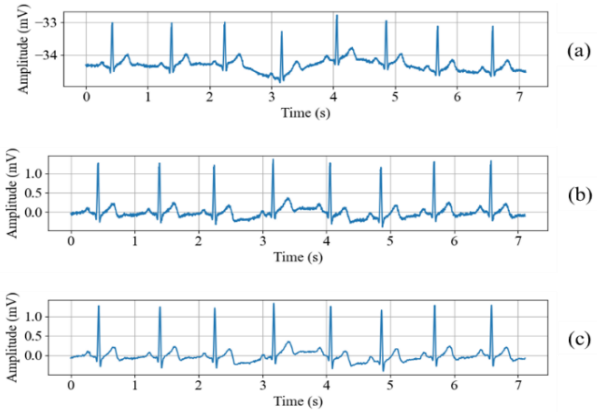

Figure 5. *Noise-filtering procedures for LII on the ESP32 (a) raw ECG signal; (b) ECG signal after high-pass filtering (HPF); (c) ECG signal after low-pass filtering (LPF)*

Figure 6 presents the results of the PT algorithm. After differentiation (Figure 6a), squaring (Figure 6b), and moving average filtering (Figure 6c), the R peak positions of the QRS complexes are clearly visible. Figure 6c shows the adaptive threshold changes applied to determine the R peak positions of the QRS complexes. Figure 6d illustrates the locations of QRS complexes on the filtered ECG data when applying equation (17) with the adaptive threshold.

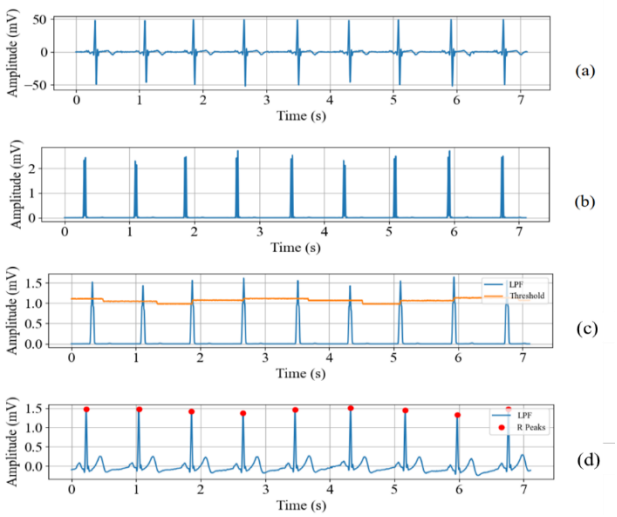

Figure 6. *Execution process of the PT algorithm on LII of self-acquired data: (a) Signal after differentiation; (b) Squared differentiated signal; (c) Signal after moving-average filtering and adaptive thresholding; (d) Filtered ECG signal and positions of detected R-peaks*

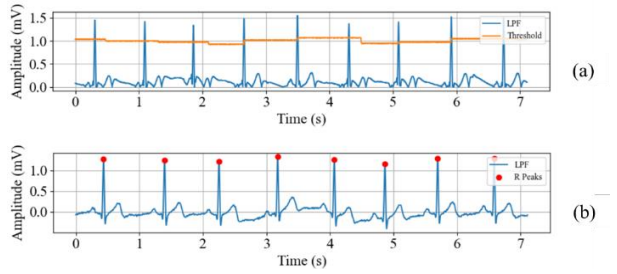

Figure 7. *Execution process of the HT algorithm on LII of acquired data: (a) Envelope signal and adaptive threshold; (b) Filtered ECG signal and positions of detected R-peaks*

Figure 7 shows the results of the HT algorithm. Despite its mathematical complexity, after extracting the ECG signal envelope (Figure 7a), the R peak positions are identified. Similarly, after applying the adaptive threshold and equation (17), the R peaks are accurately detected as shown in Figure 7b.

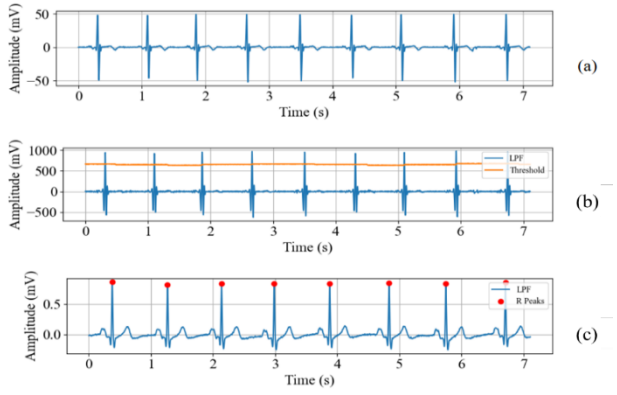

Figure 8. *xecution process of the E–Z algorithm on LII: (a) Discrete derivative signal; (b) Low-pass filtered signal and adaptive threshold; (c) Filtered ECG signal and positions of detected R-peaks*

Similar to PT and HT, the E-Z algorithm also yields highly effective real-time QRS complex identification results (Figure 8). After discrete differentiation using equation (14) and filtering with equation (15), the R peaks are highlighted (Figure 8a and 8b). Figure 8c shows the results of R peak detection of QRS complexes using the E-Z algorithm. Thus, all three algorithms were successfully implemented on the ESP32 MCU and produced very good results.

Table 1 presents a statistical comparison of QRS complex detection results for the three algorithms (PT, HT, and E-Z), including Se, +P, DER, and ACC. Specifically, PT achieved the highest sensitivity and accuracy (100%), demonstrating excellent R peak detection performance in ECG signals. HT showed sensitivity of 99.92% and accuracy of 99.46%. E-Z also achieved high sensitivity (100%) and accuracy (99.63%), indicating its effectiveness, though not as stable as PT. Therefore, in terms of accuracy, PT is the most effective algorithm when implemented on ESP32 for real-time ECG data streams. However, execution time should also be considered.

Table 1. *Summary of R-peak Detection Statistics*

Methods	Indicator	R-peak count	Standard Deviation	Min	Mean	Max
PT	Se	1470	0	100	100	100
	+P	1470	0	100	100	100
	DER	1470	0	0	0	0
	ACC	1470	0	100	100	100
HT	Se	1470	0.509	96.78	99.92	100
	+P	1470	1.491	93.54	99.54	100
	DER	1470	1.571	0	0.536	6.45
	ACC	1470	1.554	93.55	99.46	100
E-Z	Se	1470	0	100	100	100
	+P	1470	0.966	96.55	99.69	100
	DER	1470	1.002	0	0.007	3.45
	ACC	1470	1.180	94.78	99.63	100

Table 2 presents the execution time results for all three algorithms on the ESP32 MCU.

Table 2. *Algorithm Execution Time*

Task	PT	HT	E-Z
Signal preprocessing	11	115	10
Threshold	106	107	106
Total (µs)	117	222	116

The results show that HT has the highest overall execution time (222 µs), likely due to its more complex mathematical operations. This time is twice that of PT and E-Z. In contrast, PT and E-Z have similar execution times (117 µs and 116 µs, respectively), which is understandable since both use simple discrete differentiation and filtering. In summary, for the experiments in this study, PT provided the best performance in both accuracy and execution time for real-time QRS complex detection. However, these results are based on 1,470 QRS complexes on LII under optimal experimental conditions. Further experiments under different conditions are necessary to confirm the accuracy and reliability of these algorithms. Nevertheless, these are very promising results, demonstrating that these algorithms can perform well on real-time data and serve as a foundation for developing classification and diagnostic applications for cardiovascular diseases based on detected QRS complex features.

Table 3 summarizes and compares evaluation metrics (Se, +P, ACC) of reference R peak detection methods and those implemented in this study.

Table 3. *Comparative summary of R-peak detection methods*

Method	R-peak count	Se	+P	ACC
Real-time detection at the current beat [20]	110050	99.69	99.8	99.53
Pseudo-real-time detection [20]	110050	99.74	99.78	99.56
Curve-Length and Adaptive Threshold [21]	109496	99.86	99.84	99.7
Peak Threshold [18]	-	74.62	92.39	70.3
Peak Filter [18]	-	83.61	98.38	82.47
Exponential Transform and Proportional-Derivative controlled threshold [22]	109966	99.8	99.92	99.71
This study: PT	**1470**	**100**	**100**	**100**
This study: HT	**1470**	**99.92**	**99.54**	**99.46**
This study: E-Z	**1470**	**100**	**99.69**	**99.63**

4. Conclusion

In summary, this study experimentally evaluated a real-time ECG signal acquisition and processing system on a group of student volunteers, using three QRS detection algorithms: PT, HT, and E-Z. The algorithms tested in this study had a maximum execution time of 222 µs. The PT algorithm achieved the highest detection accuracy rate of 100%. The HT algorithm yielded a QRS detection accuracy of 99.46%, and the E-Z algorithm achieved 99.63%. In future work, the system will be further tested on different subjects to confirm the effectiveness of the algorithms and to propose the development of a compact device that supports clinicians and enhances public healthcare quality.

REFERENCES

[1] S. N. Qayyum, M. Iftikhar, and M. Rehan, “Revolutionizing electrocardiography : the role of artificial intelligence in modern cardiac diagnostics”, *Ann. Med. Surg.*, vol. 87, pp. 161–170, 2025.

[2] W. Lv and J. Guo, “Real-time ECG signal acquisition and monitoring for sports competition process oriented to the Internet of Things”, *Meas. J. Int. Meas. Confed.*, vol. 169, no. August 2020, 2021, doi: 10.1016/j.measurement.2020.108359.

[3] H. Ni *et al.*, “Application analysis of a new pre-localization series algorithm for differentiating wide QRS complex tachycardia”, *J. Electrocardiol.*, vol. 91, no. 1882, p. 153937, 2025, doi: 10.1016/j.jelectrocard.2025.153937.

[4] N. T. Bui and G. S. Byun, “The comparison features of ecg signal with different sampling frequencies and filter methods for real-time measurement”, *Symmetry (Basel).*, vol. 13, no. 8, 2021, doi: 10.3390/sym13081461.

[5] T. M. C. Pereira, R. C. Conceição, V. Sencadas, and R. Sebastião, “Biometric Recognition: A Systematic Review on Electrocardiogram Data Acquisition Methods”, *Sensors*, vol. 23, no. 3, pp. 1–31, 2023, doi: 10.3390/s23031507.

[6] E. Y. A. Al-Jabbar, M. M. M. Al-Hatab, M. A. Qasim, W. R. Fathel,

and M. A. Fadhil, "Clinical Fusion for Real-Time Complex QRS Pattern Detection in Wearable ECG Using the Pan-Tompkins Algorithm", *Fusion Pract. Appl.*, vol. 12, no. 2, pp. 172–184, 2023, doi: 10.54216/FPA.120214.

[7] M. N. Imtiaz and N. Khan, "Pan-Tompkins++: A Robust Approach to Detect R-peaks in ECG Signals", *Proc. - 2022 IEEE Int. Conf. Bioinforma. Biomed. BIBM 2022*, pp. 2905–2912, 2022, doi: 10.1109/BIBM55620.2022.9995552.

[8] M. Rakshit and S. Das, "An efficient wavelet-based automated R-peaks detection method using Hilbert transform", *Biocybern. Biomed. Eng.*, vol. 37, no. 3, pp. 566–577, 2017, doi: 10.1016/j.bbe.2017.02.002.

[9] B. Guénégo, C. Lelandais-perrault, E. Avignon-meseldzija, G. Sou, and P. Bénabès, "Impact of Mother Wavelet Choice on Fast Wavelet Transform Performances for Integrated ST Segment Monitoring", *Low Power Electron. Appl.*, vol. 15, no. 2, pp. 1–17, 2025.

[10] A. Lourenço, H. Silva, P. Leite, R. Lourenço, and A. Fred, "Real time electrocardiogram segmentation for finger based ECG biometrics", *BIOSIGNALS 2012 - Proc. Int. Conf. Bio-Inspired Syst. Signal Process.*, pp. 49–54, 2012, doi: 10.5220/0003777300490054.

[11] L. C. Njike Kouekeu, Y. Mohamadou, A. Djeukam, F. Tueche, and M. Tonka, "Embedded QRS complex detection based on ECG signal strength and trend", *Biomed. Eng. Adv.*, vol. 3, no. October 2021, p. 100030, 2022, doi: 10.1016/j.bea.2022.100030.

[12] V. K. Sinha and S. K. Kar, "An efficient real-time ECG QRS-complex identification by A-CLT and digital fractional order differentiation", *Biomed. Signal Process. Control*, vol. 92, no. November 2023, p. 106055, 2024, doi: 10.1016/j.bspc.2024.106055.

[13] J. Pan and W. J. Tompkins, "A Real-Time QRS Detection Algorithm", *IEEE Trans. Biomed. Eng.*, vol. BME-32, no. 3, pp. 230–236, 1985, doi: 10.1109/TBME.1985.325532.

[14] X. Lu, M. Pan, and Y. Yu, "QRS detection based on improved adaptive threshold", *J. Healthc. Eng.*, vol. 2018, 2018, doi: 10.1155/2018/5694595.

[15] A. Thomas, "Enclaves in real-time operating systems", *M.Sc. Diss. Dep. Electr. Eng. Comput. Sci. Univ. California, Berkeley, USA*, 2021.

[16] D. Benitez, P. A. Gaydecki, A. Zaidi, and A. P. Fitzpatrick, "The use of the Hilbert transform in ECG signal analysis", *Comput. Biol. Med.*, vol. 31, no. 5, pp. 399–406, 2001, doi: https://doi.org/10.1016/S0010-4825(01)00009-9.

[17] V. K. Tran, B. T. Thai, H. Pham, V. K. Nguyen, and V. K. Nguyen, "A Proposed Approach to Utilizing Esp32 Microcontroller for Data Acquisition", *J. Eng. Technol. Sci.*, vol. 56, no. 4, pp. 474–488, 2024, doi: 10.5614/j.eng.technol.sci.2024.56.4.4.

[18] T. P. Utomo, N. Nuryani, and Darmanto, "QRS peak detection for heart rate monitoring on Android smartphone", *J. Phys. Conf. Ser.*, vol. 909, no. 1, 2017, doi: 10.1088/1742-6596/909/1/012006.

[19] C. C. Lin and C. M. Yang, "Heartbeat classification using normalized RR intervals and morphological features", *Math. Probl. Eng.*, vol. 2014, 2014, doi: 10.1155/2014/712474.

[20] I. I. Christov, "Real time electrocardiogram QRS detection using combined adaptive threshold", *Biomed. Eng. Online*, vol. 3, pp. 1–9, 2004, doi: 10.1186/1475-925X-3-28.

[21] J. Lewandowski, H. E. Arochena, R. N. G. Naguib, and K.-M. Chao, "A simple real-time QRS detection algorithm utilizing curve-length concept with combined adaptive threshold for electrocardiogram signal classification", in *TENCON 2012 IEEE Region 10 Conference*, 2012, pp. 1–6. doi: 10.1109/TENCON.2012.6412176.

[22] A. Chen *et al.*, "A real time QRS detection algorithm based on ET and PD controlled threshold strategy", *Sensors (Switzerland)*, vol. 20, no. 14, pp. 1–15, 2020, doi: 10.3390/s20144003.